A numerical method for elasto-plastic notch-root stress–strain analysis

Ayhan Ince and Grzegorz Glinka

The Journal of Strain Analysis for Engineering Design 2013 48: 229 originally published online 5 April 2013
DOI: 10.1177/0309324713477638

Original Article

JSA

J Strain Analysis
48(4) 229–244

DOI: 10.1177/0309324713477638
sdj.sagepub.com
SAGE

A numerical method for elasto-plastic notch-root stress–strain analysis

Ayhan Ince and Grzegorz Glinka

Abstract

In this article, a computational modeling method of the multiaxial stress–strain notch analysis has been developed to compute elasto-plastic notch-tip stress–strain responses using linear elastic finite element results of notched components. Application and validation of the multiaxial stress–strain notch analysis model were presented by comparing computed results of the model to the experimental data of SAE 1070 steel notched shaft subjected to several nonproportional load paths. Based on the comparison between the experimental and computed strain histories, the elasto-plastic stress–strain model predicted notch strains with reasonable accuracy using linear elastic finite element stress histories. The elasto-plastic stress–strain notch analysis model provides an efficient and simple analysis method preferable to expensive experimental component tests and more complex and time-consuming incremental nonlinear finite element analysis. The elasto-plastic stress–strain model can thus be employed to perform fatigue life and fatigue damage estimates associated with the local material deformation.

Keywords

Multiaxial, elasto-plastic, stress–strain, notch analysis, nonproportional loading, cyclic plasticity, fatigue

Date received: 19 November 2012; accepted: 16 January 2013

Introduction

Fatigue failure is considered to be the most common type of failure mode experienced by most engineering components. Many mechanical components contain notches and geometrical irregularities, which cannot be avoided in practice. In addition, most of the mechanical notched components are subjected to biaxial/multiaxial loadings in services. Multiaxial loading paths produce complex stress and strain states near notches and can cause a fatigue failure at or near notch roots even without any evident large-scale plastic deformation. Therefore, notches have been considered as one of the most important problems in the design of machine components.

Local strain-based fatigue life prediction of notched components subjected to multiaxial loading paths requires detail knowledge of stresses and strains in such regions. Early researches focused primarily on determining theoretical stress concentration factors using either elasticity theory or photoelastic analysis. Peterson[1] has compiled theoretical stress concentration factors for various geometries into one book. Stowell[2] and Hardrath and Ohman[3] investigated stress concentrations in the plastic range. The most well-known approximation formula that relates the theoretical stress concentration factor to the product of the elasto-plastic stress and strain concentration factors was originally proposed by Neuber.[4] Neuber studied a semi-infinite prismatic notched body obeying a nonlinear stress and strain law. He proposed that the product of the stress and strain at the notch tip in any arbitrary notched geometry in a prismatic body is not dependent on material's nonlinear parameters but can be related to material's elastic parameters and the far field boundary conditions. Neuber's rule for uniaxial loading is

$$\sigma^a \varepsilon^a = K_t^2 Se \tag{1}$$

where σ^a and ε^a are the elasto-plastic notch-tip stress and strain, S and e are the nominal section stress and strain and K_t is the elastic stress concentration factor. Alternatively, Neuber's rule can be written in the form

$$\sigma^a \varepsilon^a = \sigma^e \varepsilon^e \tag{2}$$

Department of Mechanical and Mechatronics Engineering, University of Waterloo, Waterloo, ON, Canada

Corresponding author:
Ayhan Ince, Department of Mechanical and Mechatronics Engineering, University of Waterloo, 200 University Avenue West, Waterloo, ON, Canada N2L 3G1.
Email: ayhan.ince@yahoo.com

where $\sigma^e = K_t S$ and $\varepsilon^e = K_t e$ are the fictitious elastic strain and stress. Equation (2) states that the total strain energy density and complementary energy density at the notch tip are equal to the fictitious strain energy density and complementary energy density as if a material hypothetically remained elastic.

Topper et al.[5] extended validation of Neuber's rule to several notch geometries subjected to uniaxial cyclic loading. Their results showed that Neuber's rule for cyclic loading was in good agreement with experimental results for notched aluminum alloy sheets. Molski and Glinka[6] proposed the equivalent strain energy density (ESED) method as an alternative to Neuber's rule. They postulated that the strain energy density at a notch equals that if the body were to hypothetically remain elastic. The authors showed[6] that the ESED method provided good agreement with experiment for several notched specimens subjected to monotonic loading. The ESED method can be written in terms of stresses and strains as

$$\frac{1}{2}\sigma^e\varepsilon^e = \int_0^{\varepsilon^a} \sigma^a d\varepsilon^a \tag{3}$$

Glinka[7] later extended the ESED method to address notched bodies subjected to cyclic loading. As the local strain-life approach was extended to multiaxial loading using multiaxial fatigue damage parameters, these damage parameters require multiaxial strains and stresses to be determined at notch areas. Since nonlinear finite element analysis (FEA) is too costly to compute multiaxial stresses and strains for a long load history, simple uniaxial notch stress and strain approximation techniques were extended to states of multiaxial stress and strain. Hoffmann and Seeger[8,9] proposed a method for multiaxial proportional loading by applying an equivalent form of Neuber's rule as

$$\sigma^a_{eq}\varepsilon^a_{eq} = \sigma^e_{eq}\varepsilon^e_{eq} \tag{4}$$

where σ^a_{eq} and ε^a_{eq} are the notch-tip elastic–plastic equivalent stress and strain, respectively, and σ^e_{eq} and ε^e_{eq} are those that would be obtained if the material remained elastic. They assumed that the ratio of minimum principal strain components at the notch tip remains constant during loading.

Ellyin and Kujawski[10] proposed a method that the maximum stress and strain at the notch roots can be calculated for monotonic and cyclic loadings from the knowledge of the theoretical stress concentration factor K_t. This method is based on an averaged similarity measure of the stress and strain energy densities along a smooth notch boundary. The method can also be used in the case of multiaxial states of stress. Ellyin and Kujawski reported that the predicted stresses and strains at the notch root were in good agreement with the available experimental data and FE results. The generalization of both the ESED method and Neuber's rule for proportional multiaxial loading for notched bodies was suggested by Moftakhar.[11] Numerical and experimental studies conducted by Moftakhar et al.[12] showed that the generalized ESED method and Neuber's rule provide upper and lower bounds of the actual strains. Their study concluded that Neuber's rule tends to overestimate the notch-tip elastic–plastic strains and stresses and the ESED method tends to underestimate the notch-tip inelastic strains and stresses. Hoffman et al.[13] presented a method to estimate notch-root stresses and strains for bodies subjected to nonproportional loading. In their method, the multiaxial loads are first separated and notch-root strain histories are calculated for the loads independently by following the same solution procedure as for proportional loading. Compatibility iteration is then used to account for interaction between strain components that result from nonproportional loading. Their calculations compared well with FEA. Barkey[14] and Barkey et al.[15] later proposed a method to estimate multiaxial notch strains in notched bars subject to cyclic proportional and nonproportional loading, using the concept of a structural yield surface. The structural yield surface describes the relationship between nominal stresses and notch strains. The hardening parameter is found by using the uniaxial form of the ESED method as the basis of nominal load to notch plastic strain curve. Their results showed good agreement with experimental nonproportional tension–torsion tests for a notched steel bar. Köttgen et al.[16] extended Barkey's approach by incorporating the notch effect into the constitutive relation. They first obtained pseudo stress history by assuming elastic material behavior. The yield criterion and the flow rule were determined using elastic stress history, and the hardening parameter was determined using pseudo stress and local plastic strain curve obtained from a uniaxial simplified rule. The resulting elastic–plastic strain increments were then fed back into the flow rule to calculate notch stresses. Köttgen et al. reported correlation of their method with elasto-plastic FEA for various geometries and applied loads. Singh[17] extended the ESED and Neuber's methods to estimate the notch-root stresses and strains for monotonic nonproportional loading. The approach is an incremental generalization of the ESED method and Neuber's rule. In generalizing the ESED method, Singh suggested that for a given increment of external load, the corresponding increment of the strain energy density at the notch tip in an elastic–plastic body is equal to the increment of the strain energy density if the body were to remain elastic.

Recent research studies[18–20] have shown that the notch correction method can be combined with the cyclic plasticity model to compute the local stress and strain history from the pseudo-elastic stress and strain at the notch area. Coupling the notch correction method and the cyclic plasticity to compute the local stresses and strains at critical locations in components provides a great advantage over experiments and incremental elastic–plastic FEAs due to its simplicity,

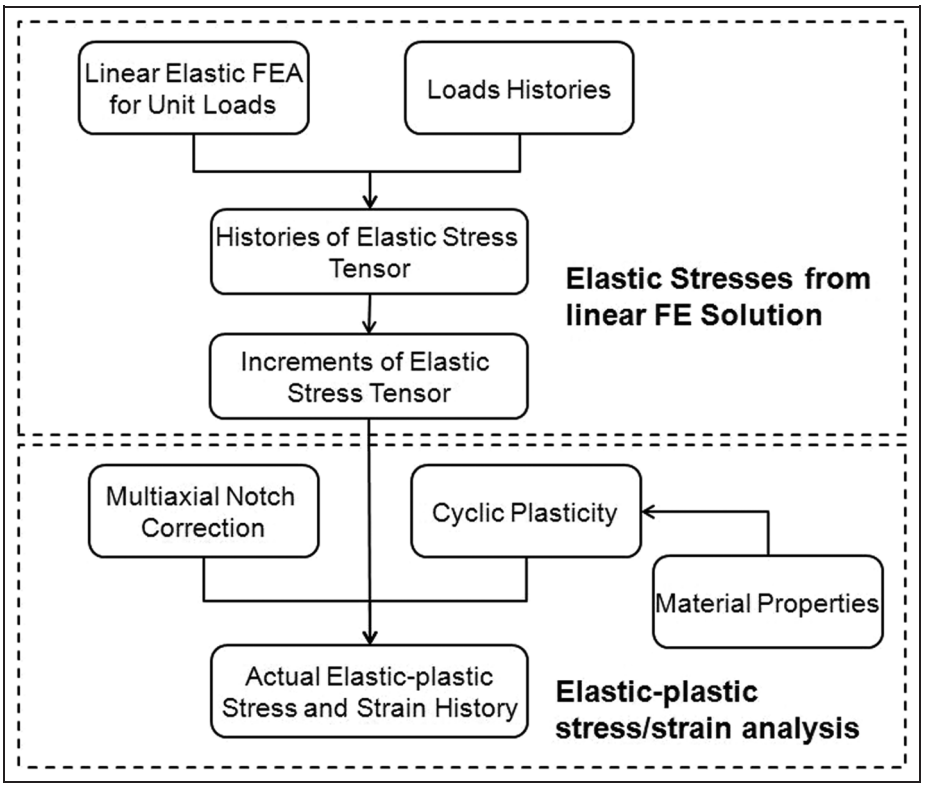

Figure 1. Algorithm for notch stress and strain analyses.
FEA: finite element analysis.

computational efficiency, low cost and reasonable accuracy. The multiaxial stress–strain notch analysis method originally proposed by Buczynski and Glinka[19] is adapted to develop the elastic–plastic stress–strain model to compute local stress–strain responses using linear elastic FE results of notched components. A general numerical algorithm is developed on the basis of incremental relationships, which relate the elastic and elastic–plastic strain energy densities at the notch root and the material stress–strain behavior, simulated by the Garud[21] cyclic plasticity model. The algorithm computes multiaxial elasto-plastic stress–strain responses for many nodal points that define critical notch areas of the FE model. A flowchart for the algorithm implementing the stress and strain analyses for notched components subjected to the multiaxial loadings is shown in Figure 1.

Linear elastic stress–strain histories

FE models are used often to analyze engineering components. A linear elastic FEA can be used to calculate linear elastic stresses/strains for a notched component. Once the elastic stresses/strains are known, the elasto-plastic stress–strain analysis (combined with the multiaxial notch correction and the cyclic plasticity) can be used to compute the actual elastic–plastic stress and strain responses at notch areas. The linear elastic FEA assumes that there is a linear relationship between the applied external load and stress–strain results. Axle and shaft components often experience combined bending and torsion loads. Let us consider a notched shaft shown in Figure 2, which has two applied load histories, namely, bending and torque. The FEA is performed to calculate unit-load linear elastic stress tensors for each applied load. The elastic stress tensor at each node from the linear elastic FEA is multiplied by the corresponding load history to compute a time history of elastically calculated stress tensor. If the elastic stress tensor at a node is σ_{ij}^{ep} for a unit load of p, the time history of the elastic stress tensor $\sigma_{ij}^{eP(t)}$ for the load history $P(t)$ can be calculated as

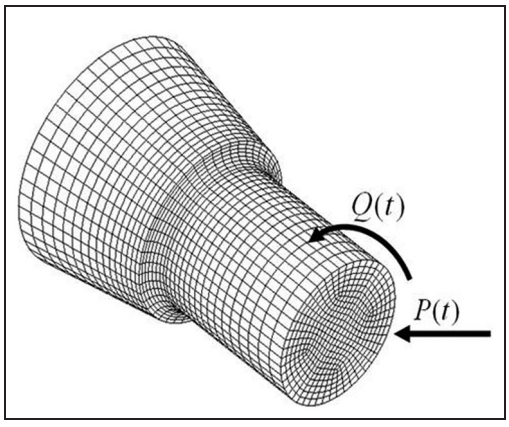

Figure 2. A notched shaft with applied load histories $P(t)$ and $Q(t)$.

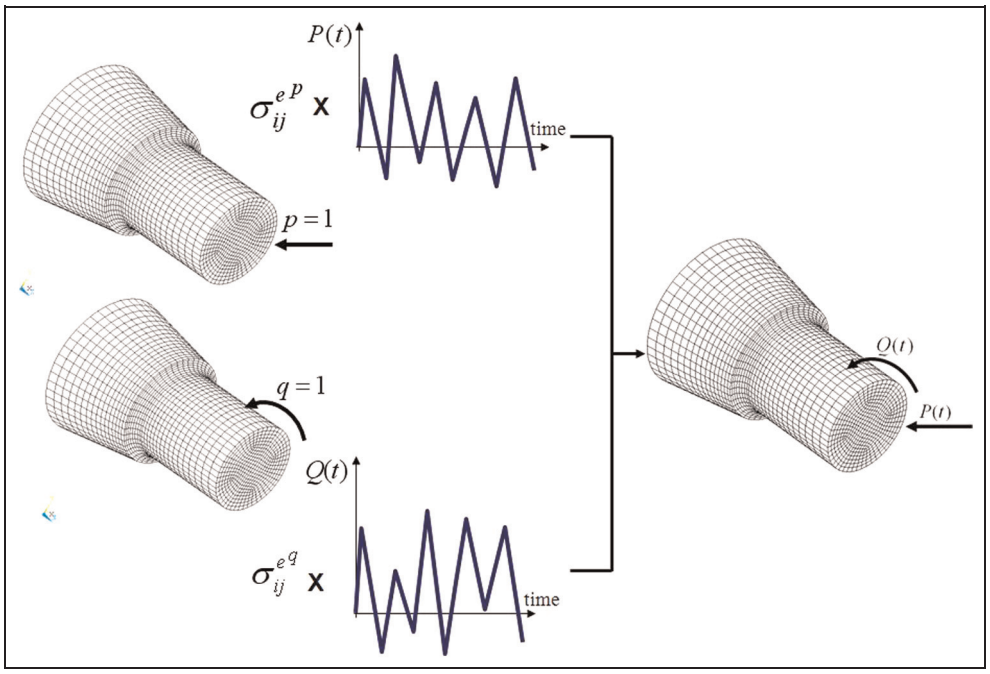

Figure 3. Superimposing FEA elastic stress results from two load histories.

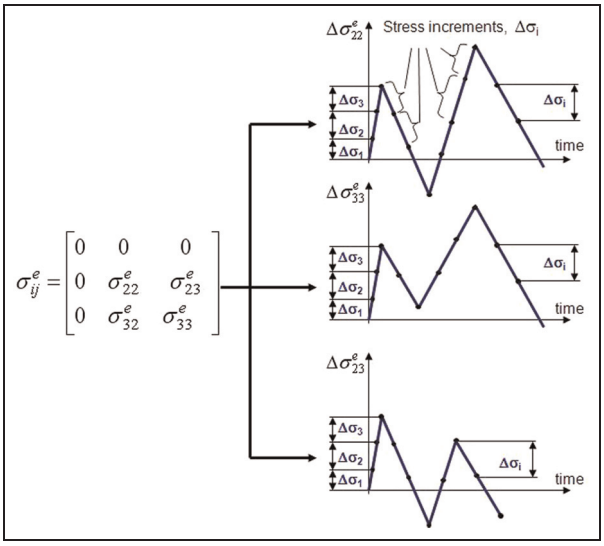

Figure 4. The input elastic stress increments of the time history of the stress.

$$\sigma_{ij}^{eP(t)} = P(t)\sigma_{ij}^{ep} \tag{5}$$

If the elastic stress tensor at the same node is σ_{ij}^{eq} for a unit load of q, the time history of the elastic stress tensor $\sigma_{ij}^{eQ(t)}$ for the load history $Q(t)$ can be calculated as

$$\sigma_{ij}^{eQ(t)} = Q(t)\sigma_{ij}^{eq} \tag{6}$$

Time histories of elastic stress tensors $\sigma_{ij}^{eP(t)}$ and $\sigma_{ij}^{eQ(t)}$ for the same node are then superimposed to obtain the resultant time history of the elastic stress tensor for both load histories $P(t)$ and $Q(t)$, applied simultaneously

$$\sigma_{ij}^{e} = \sigma_{ij}^{eP} + \sigma_{ij}^{eQ} \tag{7}$$

Figure 3 shows a schematic representation of the implementation procedure for superimposing elastic stress tensors. Since fatigue crack initiation is formed on the surface of a component, elastic stress tensors for surface nodes at critical notch areas are used for estimating actual elastic–plastic stress–strain responses. A macro routine written in ANSYS Parametric Design Language (APDL) is used to compute elastic stress results for surface nodes for each unit load. Unit-load elastic stress results from the FEA and corresponding time histories for each unit load are used as input to a computer program to calculate combined time histories of elastic stress tensor at critical notch areas.

If components of a stress tensor change proportionally during the loading, the loading is called proportional. When the applied load results in the change of the principal stress directions and the ratio of the principal stresses, the loading is called nonproportional. When plastic yielding takes place at the notch tip, then the stress path at the notch-tip region is usually nonproportional regardless of whether the external loading is proportional or not. Nonproportional loading/stress paths are usually defined by increments of load/stress components, and therefore, stress–strain calculations have to be carried out in incremental form. Time histories of elastic stresses are transformed to increments of elastic stresses. A schematic representation of elastic stress increments used as input to the stress–strain notch analysis model is shown in Figure 4.

For the case of general multiaxial loading applied to a notched body, the state of stress near the notch tip is triaxial. However, the stress state at the notch tip is

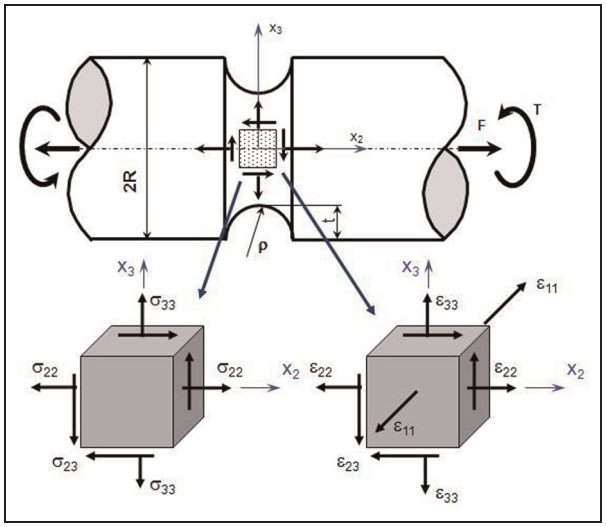

Figure 5. Stress and strain states at a notch tip.

biaxial because of the notch-tip stress for a free surface as shown in Figure 5. Since equilibrium of the infinitesimal element at the notch tip must be maintained, that is, $\sigma^e_{23} = \sigma^e_{32}$ and $\varepsilon^e_{23} = \varepsilon^e_{32}$, there are three nonzero stress components and four nonzero strain components (Figure 5)

$$\sigma^e_{ij} = \begin{bmatrix} 0 & 0 & 0 \\ 0 & \sigma^e_{22} & \sigma^e_{23} \\ 0 & \sigma^e_{32} & \sigma^e_{33} \end{bmatrix} \quad \text{and} \quad \varepsilon^e_{ij} = \begin{bmatrix} \varepsilon^e_{11} & 0 & 0 \\ 0 & \varepsilon^e_{22} & \varepsilon^e_{23} \\ 0 & \varepsilon^e_{32} & \varepsilon^e_{33} \end{bmatrix} \tag{8}$$

Seven fictitious linear elastic stress and strain components ($\sigma^e_{ij}, \varepsilon^e_{ij}$) are obtained from the linear elastic FE solution; however, the actual elastic–plastic stress and strain components ($\sigma^a_{ij}, \varepsilon^a_{ij}$) at the notch tip are unknown. Therefore, a set of seven independent equations are required for the calculation of actual elastic–plastic stress and strain components at the notch tip. The multiaxial Neuber notch correction rule and the Garud cyclic plasticity model are integrated to provide the required seven equations to solve for all unknown stress and strain components. The cyclic plasticity provides four equations, and the notch correction rule provides the remaining three equations.

Constitutive governing equations

Under applied cyclic loadings, stress–strain responses at critical regions (notches) often show a transient response but stabilize over a number of cycles. For nonproportional load histories, an incremental plasticity analysis is required to estimate the material's stress–strain response. A number of incremental plasticity models[21–27] have been developed to estimate constitutive material behavior, and some of those models are sophisticated to include the transient hardening responses. However, these complex models require significant material testing to characterize model parameters and are not appropriate for practical engineering use. Furthermore, for the multiaxial fatigue analysis, the transient nature of deformation behavior is not as critical as the behavior of cyclically stabilized material behavior. Therefore, a relatively simple Garud hardening model is used to deal with proportional and nonproportional multiaxial loadings.

The cyclic plasticity model provides a set of governing equations to relate stress and strain components. Since the fatigue cracks most often initiate on the surface of a component, governing equations are provided for stress–strain state on the free component surface. Governing equations are presented in deviatoric space based on a rate-independent, homogenous and isotropic material because it is easier to formulate the equations using deviatoric stress and strain quantities.

In elastic loadings, the deformation process is reversible, and when the applied load is removed from the body, the deformed body returns to its original state. There is a direct relationship between stress and strain, and relations between stress and strain tensors are determined by Hooke's law (equation (9)).

The generalized Hooke's law in an incremental form is represented as

$$d\varepsilon^e_{ij} = \frac{1+v}{E} d\sigma_{ij} - \frac{v}{E} d\sigma_{ij}\delta_{ij} \tag{9}$$

When the body is deformed beyond the material's yield limit, permanent plastic deformation occurs, and the deformation process becomes irreversible. When the applied load is removed from the body, the permanent deformation remains in the body. Based on the plasticity theory, the stress and strain states are dependent on the loading path. As well known, there are three main elements required in order to model constitutive behavior of the material: a yield criterion, which defines a boundary between elastic and elastic–plastic stress states; a flow rule, which describes the relationship between stress and strain increments; and a hardening rule, which describes how yield function changes during the plastic deformation. The von Mises yield criterion has been the most popular criterion for modeling the material constitutive behavior. Since it is widely accepted that hydrostatic stresses do not influence yielding, the yield function, equation (10), for the isotropic hardening can be described as a uniform and symmetrical expansion of the yield surface in all directions during plastic loading

$$F = \frac{3}{2} S_{ij} S_{ij} - \sigma^2_y(k) = 0 \tag{10}$$

where S_{ij} is the deviatoric stress tensor and $\sigma_y(k)$ is the current size of the yield surface as a function of k.

The yield function, equation (11), for the kinematic hardening can be represented as a translation of the yield surface without any expansion during plastic loading. The yield surface for the kinematic hardening maintains its shape and size

$$F = \frac{3}{2}(S_{ij} - a_{ij})(S_{ij} - a_{ij}) - \sigma_{yo}^2 = 0 \tag{11}$$

The flow rule, equation (12), defines the relationship between stress and plastic strain increments. The flow rule, based on the normality postulate by Drucker,[22] implies that the increment of plastic strain is in the normal direction to the yield surface during plastic deformation

$$d\varepsilon_{ij}^p = d\lambda \frac{\partial F}{\partial \sigma_{ij}} \tag{12}$$

where $d\varepsilon_{ij}$ is the plastic strain increment tensor, σ_{ij} is the stress tensor, F is the yield function, and $d\lambda$ is a scalar-valued function.

For elastic–plastic loading, total strain tensor is the sum of elastic strain determined by Hooke's law and plastic strain determined by the flow rule

$$\varepsilon_{ij} = \varepsilon_{ij}^e + \varepsilon_{ij}^p \tag{13}$$

Similarly, the elastic and plastic strain increment can be added to obtain the total strain increment

$$d\varepsilon_{ij} = d\varepsilon_{ij}^e + d\varepsilon_{ij}^p \tag{14}$$

Substituting equations (9) and (12) into equation (14) yields a general form of the total elastic–plastic strain increment. The generalized constitutive elasto-plastic stress–strain relationships are derived from the uniaxial stress–strain curve by using principles of the theory of elasticity and plasticity

$$d\varepsilon_{ij} = \frac{1+v}{E} d\sigma_{ij} - \frac{v}{E} d\sigma_{ij}\delta_{ij} + d\lambda \frac{\partial F}{\partial \sigma_{ij}} \tag{15}$$

In the case of proportional stress path, the Hencky total deformation of plasticity equations can be used for stress–strain analysis

$$\varepsilon_{ij}^a = \frac{1+v}{E}\sigma_{ij}^a - \frac{v}{E}\sigma_{kk}^a\delta_{ij} + \frac{3}{2}\frac{\varepsilon_{eq}^{pa}}{\sigma_{eq}^a} \cdot S_{ij}^a \tag{16}$$

The normality flow rule, also called the Prandtl–Reuss relation, is considered one of the most frequently used model in the incremental plasticity. The total strain increment, equation (15), can be expressed in the form of the Prandtl–Reuss strain–stress relationship

$$\Delta\varepsilon_{ij}^a = \frac{1+v}{E}\Delta\sigma_{ij}^a - \frac{v}{E}\Delta\sigma_{kk}^a\delta_{ij} + \frac{3}{2}\frac{\Delta\varepsilon_{eq}^{pa}}{\sigma_{eq}^a} \cdot S_{ij}^a \tag{17}$$

The notch-tip deviatoric stresses of the hypothetical linear elastic body are determined as

$$S_{ij}^e = \sigma_{ij}^e - \frac{1}{3}\sigma_{kk}^e\delta_{ij} \tag{18}$$

The elastic deviatoric strain and stress increments can be calculated from Hooke's law

$$\Delta e_{ij}^e = \frac{\Delta S_{ij}^e}{2G} \tag{19}$$

The actual deviatoric stress components in the notch tip can analogously be defined as

$$S_{ij}^a = \sigma_{ij}^a - \frac{1}{3}\sigma_{kk}^a\delta_{ij} \tag{20}$$

The incremental deviatoric stress–strain relations based on the associated Prandtl–Reuss flow rule can be subsequently written as

$$\Delta e_{ij}^a = \frac{\Delta S_{ij}^a}{2G} + d\lambda \cdot S_{ij}^a \tag{21}$$

where

$$\frac{1}{2G} = \frac{1+\nu}{E}, \quad d\lambda = \frac{3}{2}\frac{\Delta\varepsilon_{eq}^p}{\sigma_{eq}^a}, \quad \sigma_{eq}^{a2} = \frac{3}{2}S_{ij}^a S_{ij}^a,$$

$$\Delta\varepsilon_{eq}^p = \frac{df(\sigma_{eq}^a)}{d\sigma_{eq}^a}\Delta\sigma_{eq}^a$$

This relation assumes that the plastic strain increments at any instant of loading are proportional to the deviatoric stress components. The relation between the equivalent plastic strain increment and the equivalent stress increment in the uniaxial stress–strain curve can be used to determine the multiaxial incremental stress–strain relation

$$\Delta\varepsilon_{eq}^{pa} = \frac{\Delta\sigma_{eq}^a}{E_T^p} \tag{22}$$

where $\Delta\varepsilon_{eq}^{pa}$ is the equivalent plastic strain increment, $\Delta\sigma_{eq}^a$ is the equivalent stress increment and E_T^p is the current value of the generalized plastic modules.

The function $\Delta\varepsilon_{eq}^{pa} = f\left(\Delta\sigma_{eq}^a\right)$ is identical to the plastic strain–stress relationship obtained experimentally from uniaxial tension test. The plastic strain–stress relationship can be expressed according to the uniaxial Ramberg–Osgood equation

$$\sigma = K'(\varepsilon^p)^{n'} \tag{23}$$

where the constants K' and n' are determined by uniaxial tensile test.

The analytical expression of the generalized plastic modules E_T^p can be derived using the Ramberg–Osgood equation

$$E_T^p = \frac{2}{3}\frac{d\sigma}{d\varepsilon^p} = \frac{2}{3}E^p = \frac{2}{3}K'n'\left(\frac{\sigma}{K'}\right)^{\frac{n'-1}{n'}} \tag{24}$$

where E^p is the slope of the uniaxial stress–plastic strain curve (or the uniaxial plastic modulus).

The uniaxial stress–strain curve is divided into a number of stress fields (Figure 6). Each stress surface defines regions with constant plastic modulus in the stress space. Figure 6 shows a graphic interpretation of generalizations of the $\sigma_{eq} - \varepsilon_{eq}^p$ curve in the stress space and stress fields of constant plastic modules.

In the case of stress and strain states on the free surface of the notch, material constitutive equations are given in terms of deviatoric stresses as

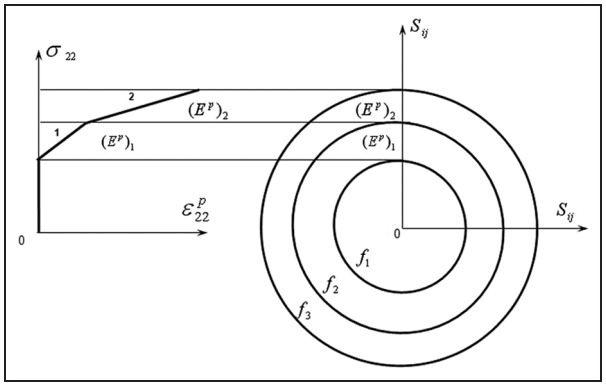

Figure 6. A graphical representation of fields of constant plastic modules and the multilinear material curve.

$$\begin{aligned}
\Delta e^a_{11} &= \frac{\Delta S^a_{11}}{2G} + d\lambda \cdot S^a_{11} \\
\Delta e^a_{22} &= \frac{\Delta S^a_{22}}{2G} + d\lambda \cdot S^a_{22} \\
\Delta e^a_{33} &= \frac{\Delta S^a_{33}}{2G} + d\lambda \cdot S^a_{33} \\
\Delta e^a_{23} &= \frac{\Delta S^a_{23}}{2G} + d\lambda \cdot S^a_{23}
\end{aligned} \tag{25}$$

Four notch strain increments (Δe^a_{11}, Δe^a_{22}, Δe^a_{33}, Δe^a_{23}) and three notch stress increments ($\Delta\sigma^a_{22}$, $\Delta\sigma^a_{33}$, $\Delta\sigma^a_{23}$) in equation (25) form seven unknowns to be solved. Four deviatoric stress increments (ΔS^a_{11}, ΔS^a_{22}, ΔS^a_{33}, ΔS^a_{23}) in equation (25) are functions of three notch stress increments ($\Delta\sigma^a_{22}$, $\Delta\sigma^a_{33}$, $\Delta\sigma^a_{23}$).

Coupling constitutive equations and Neuber's notch correction relation

The main goal of this section is to show how to combine a cyclic plasticity model and notch correction method to determine a set of governing equations to compute the notch stress and strain components.

The load is usually represented by the nominal stress being proportional to the remote loading for notched bodies. In the case of notched bodies in a plane stress or plane strain state, the relationship between the elastic notch-tip stresses and strains and the actual elastic–plastic notch-tip stresses and strains in the localized plastic zone is often approximated by the Neuber rule or the ESED method. It was shown[17,19] that both methods can also be extended for multiaxial proportional and nonproportional modes of loading. Similar approaches were proposed by Hoffman and Seeger[13] and Barkey.[14] All methods consist of two parts, namely, the constitutive equations and the notch correction relating the pseudo-linear elastic stress–strain state (σ^e_{22}, ε^e_{22}) at the notch tip with the actual elastic–plastic stress–strain response (σ^a_{22}, ε^a_{22}).

The Neuber rule[4] for proportional loading, where the Hencky stress–strain relationships are applicable, can be written for the uniaxial and multiaxial stress states in the form of equations (26) and (27), respectively

$$\sigma^e_{22}\,\varepsilon^e_{22} = \sigma^a_{22}\,\varepsilon^a_{22} \tag{26}$$

$$\sigma^e_{ij}\,\varepsilon^e_{ij} = \sigma^a_{ij}\,\varepsilon^a_{ij} \tag{27}$$

The ESED method[6] represents the equality between the strain energy density at the notch tip of a linear elastic body and the notch-tip strain energy density of a geometrically identical elastic–plastic body subjected to the same load. The strain energy density equations for the ESED method for the uniaxial and multiaxial stress states can be written in the form of equations (28) and (29), respectively

$$\int_0^{\varepsilon^e_{22}} \sigma^e_{22} d\varepsilon^e_{22} = \int_0^{\varepsilon^a_{22}} \sigma^a_{22} d\varepsilon^a_{22} \tag{28}$$

$$\int_0^{\varepsilon^e_{ij}} \sigma^e_{ij} d\varepsilon^e_{ij} = \int_0^{\varepsilon^a_{ij2}} \sigma^a_{ij} d\varepsilon^a_{ij} \tag{29}$$

The strain energy density equality, equations (27) and (29), relating the pseudo-elastic and the actual elastic–plastic notch strains and stresses at the notch tip, has been widely used as a good approximation method, but additional conditions are required for the complete solution of a multiaxial stress state problem. However, those conditions have been the subject of controversy. Hoffman and Seeger[13] assumed that the ratio of the actual principal strains at the notch tip is equal to the ratio of the fictitious elastic principal strain components, while Barkey[14] suggested using the ratio of principal stresses. Barkey's approach was based on assumptions that if the applied loads are proportional, the notch-tip deviatoric stress components remain in fixed proportion, and if the applied loads are nonproportional, the ratio of the normal stresses remains in fixed proportional during the loading history. These assumptions are sufficiently accurate in the case of circumferential notches for cylindrical bodies but are not true in general multiaxial loading. Moftakhar[11] found that the accuracy of the stress or strain ratio–based analysis depended on the degree of constraint at the notch tip. Therefore, Moftakhar et al. proposed[12] to use the ratios of strain energy density contributed by each pair of corresponding stress and strain components. Singh[17] confirmed later that the additional energy equations provide a good accuracy when used in an incremental form. Because the ratios of strain energy density increments seem to be less dependent on the geometry and constraint conditions at the notch tip than the ratios of stresses or strains, the analyst is not forced to make any arbitrary decision about the constraint while using these equations. It was also found that the conflict between the plasticity model (normality rule) and strain energy density equations at some specific ratios of stress components may cause singularity for a set of seven equations. Such a conflict can be

avoided if the principal idea of Neuber is implemented in the incremental form. It should be noted that the original Neuber rule was derived for bodies in pure shear stress state. It means that the Neuber equation states the equivalence of only distortional strain energies. In order to formulate the set of necessary equations for a multiaxial analysis of elastic–plastic stresses and strains at the notch tip, the equality of increments of the total distortional strain energy density should be used. Therefore, a set of seven equations from the normality rule and strain energy density should be formulated in a deviatoric stress space to be consistent with the original Neuber rule. However, Moftakhar et al.[12] and Singh[17] suggested these equations in the normal stress space. Thus, the equations were overconstrained due to inclusion of hydrostatic stress components in the solution.

Buczynski and Glinka[19] proposed, analogous to the original Neuber rule, to use the equivalence of increments of the total distortional strain energy density contributed by each pair of associated stress and strain components, that is

$$\begin{aligned} S^{e}_{22}\Delta e^{e}_{22} + e^{e}_{22}\Delta S^{e}_{22} &= S^{a}_{22}\Delta e^{a}_{22} + e^{a}_{22}\Delta S^{a}_{22} \\ S^{e}_{33}\Delta e^{e}_{33} + e^{e}_{33}\Delta S^{e}_{33} &= S^{a}_{33}\Delta e^{a}_{33} + e^{a}_{33}\Delta S^{a}_{33} \\ S^{e}_{23}\Delta e^{e}_{23} + e^{e}_{23}\Delta S^{e}_{23} &= S^{a}_{23}\Delta e^{a}_{23} + e^{a}_{23}\Delta S^{a}_{23} \end{aligned} \tag{30}$$

The equalities of strain energy increments for each set of corresponding hypothetical elastic and actual elastic–plastic strains and stress increments at the notch tip can be shown graphically in Figure 7. The area of dotted rectangles represents the total strain energy increment of the hypothetical elastic notch-tip input stresses, while the area of the hatched rectangles represents the total strain energy density of the actual elastic–plastic material response at the notch tip.

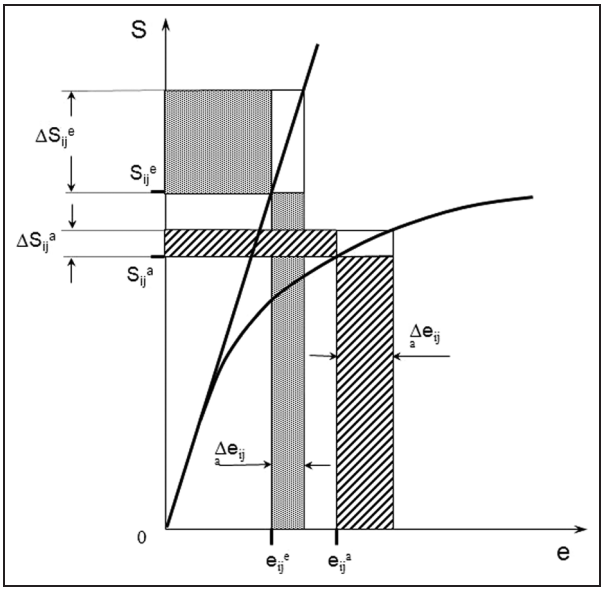

Figure 7. Graphical representation of the incremental Neuber rule.

Consequently, a combination of four equations from the elastic–plastic constitutive equation (25) and three equations from the equivalence of increments of the total distortional strain energy density, equation (30), yields the required set of seven independent equations necessary to completely define elastic–plastic notch-tip strain and stress responses for a notched component subjected to multiaxial nonproportional cyclic loads. The final set of equations written as a set of seven simultaneous equations, equation (31), from which all unknown deviatoric strain, Δe^{a}_{ij}, and stress, ΔS^{a}_{ij}, increments can be calculated, based on the linear hypothetical elastic notch-tip stress history, that is, increments $\Delta\sigma^{e}_{ij}$ and Δe^{e}_{ij}, are known from the linear elastic FEA

$$\begin{aligned} \Delta e^{a}_{11} &= \frac{\Delta S^{a}_{11}}{2G} + \frac{3}{2}\frac{\Delta\sigma^{a}_{eq}}{E^{p}_{T}\sigma^{a}_{eq}}\cdot S^{a}_{11} \\ \Delta e^{a}_{22} &= \frac{\Delta S^{a}_{22}}{2G} + \frac{3}{2}\frac{\Delta\sigma^{a}_{eq}}{E^{p}_{T}\sigma^{a}_{eq}}\cdot S^{a}_{22} \\ \Delta e^{a}_{33} &= \frac{\Delta S^{a}_{33}}{2G} + \frac{3}{2}\frac{\Delta\sigma^{a}_{eq}}{E^{p}_{T}\sigma^{a}_{eq}}\cdot S^{a}_{33} \\ \Delta e^{a}_{23} &= \frac{\Delta S^{a}_{23}}{2G} + \frac{3}{2}\frac{\Delta\sigma^{a}_{eq}}{E^{p}_{T}\sigma^{a}_{eq}}\cdot S^{a}_{23} \\ S^{e}_{22}\Delta e^{e}_{22} + e^{e}_{22}\Delta S^{e}_{22} &= S^{a}_{22}\Delta e^{a}_{22} + e^{a}_{22}\Delta S^{a}_{22} \\ S^{e}_{33}\Delta e^{e}_{33} + e^{e}_{33}\Delta S^{e}_{33} &= S^{a}_{33}\Delta e^{a}_{33} + e^{a}_{33}\Delta S^{a}_{33} \\ S^{e}_{23}\Delta e^{e}_{23} + e^{e}_{23}\Delta S^{e}_{23} &= S^{a}_{23}\Delta e^{a}_{23} + e^{a}_{23}\Delta S^{a}_{23} \end{aligned} \tag{31}$$

Since the equation set (31) is linear, the solution of the equations requires the Gaussian elimination approach. For each increment of the external load, represented by the increments of pseudo-elastic deviatoric stresses ΔS^{e}_{ij}, the deviatoric elastic–plastic notch-tip strain and stress increments Δe^{a}_{ij} and ΔS^{a}_{ij} are computed from equation (31). The calculated deviatoric stress increments ΔS^{a}_{ij} can subsequently be converted into the actual stress increments $\Delta\sigma^{a}_{ij}$ using equation (32)

$$\begin{aligned} \Delta S^{a}_{22} &= \Delta\sigma^{a}_{22} - \frac{1}{3}\left(\Delta\sigma^{a}_{22} + \Delta\sigma^{a}_{33}\right) \\ \Delta S^{a}_{33} &= \Delta\sigma^{a}_{33} - \frac{1}{3}\left(\Delta\sigma^{a}_{22} + \Delta\sigma^{a}_{33}\right) \\ \Delta S^{a}_{23} &= \Delta\sigma^{a}_{23} \end{aligned} \tag{32}$$

The deviatoric and the actual stress components S^{a}_{ij} and σ^{a}_{ij} at the end of given load increment are determined from equations (33) and (34)

$$S^{an}_{ij} = S^{ao}_{ij} + \sum_{k=1}^{n-1}\Delta S^{ak}_{ij} + \Delta S^{an}_{ij} \tag{33}$$

$$\sigma^{an}_{ij} = \sigma^{ao}_{ij} + \sum_{k=1}^{n-1}\Delta\sigma^{ak}_{ij} + \Delta\sigma^{an}_{ij} \tag{34}$$

where n denotes the load increment number.

The actual strain increments $\Delta\varepsilon^{a}_{ij}$ can finally be determined from equation (25). Before the solution of plasticity equations, loading/unloading conditions must be

checked. At the beginning of initial loading cycle, it is assumed that all strains/stresses are elastic, and the notch-tip stress–strain response is equal to the known elastic solution, equation (9)

$$\sigma_{ij}^{a} = \sigma_{ij}^{e}$$
$$\varepsilon_{ij}^{a} = \varepsilon_{ij}^{e} \tag{35}$$

When the elastic loading reached the initial yield surface, subsequent load increment may result in elastic unloading, tangential (neutral) loading and elastic–plastic (active) loading. The mode of loading is determined based on the loading criterion. When the stress increment moves inward from the yield surface, elastic unloading will take place, that is, the inner product of tensors dS, $\partial F/\partial S$, satisfies the condition

$$\frac{\partial F}{\partial S_{ij}} dS_{ij} < 0 \tag{36}$$

If the stress increment is tangential to the yield surface, the neutral loading will occur, that is, the inner product of tensors dS, $\partial F/\partial S$, satisfies the condition

$$\frac{\partial F}{\partial S_{ij}} dS_{ij} = 0 \tag{37}$$

Since the computer implementation of the neutral loading is virtually impossible to determine, this loading criterion is regarded as an elastic unloading. The relevant constitutive relations for the elastic unloading and tangential loading are described based on Hooke's law, equation (9). When the current state of stress increments moves out from the yield surface, the elastic–plastic loading will take place, that is, the inner product of tensors dS, $\partial F/\partial S$, satisfies the condition

$$\frac{\partial F}{\partial S_{ij}} dS_{ij} > 0 \tag{38}$$

The elastic–plastic loading condition states that the projection of the stress increment onto the normal of the yield surface must be greater than zero. The relevant constitutive relations for the elastic–plastic loading are described based on Hooke's law and Prandtl–Reuss equation (17).

Substituting the yield surface equation (11) for kinematic hardening into these loading criteria, the loading mode criterion LC, in terms of finite increments can be written for the purpose of numerical implementation as follows

$$LC = \sum_{i=2,3}^{j=2,3} (S_{ij}^{a} - \alpha_{ij}^{n}) \Delta\sigma_{ij}^{e} \tag{39}$$

The loading mode criterion LC, for the incremental Neuber method states that elastic unloading or the elastic–plastic loading takes place as

$$LC \leqslant 0 \quad \textit{Elastic Unloading}$$
$$LC > 0 \quad \textit{Elastic}-\textit{Plastic Loading} \tag{40}$$

The coupled constitutive governing and Neuber's incremental equations discussed before are related with the Garud cyclic plasticity model to compute the actual notch-tip stress–strain response of a notched component subjected to proportional and nonproportional multiaxial cyclic loading. After the notch stress increments are determined, the translation of the yield surface is updated by employing the multisurface hardening model proposed by Garud.[21]

Cyclic plasticity model

In order to estimate the elasto-plastic stress and strain responses at critical notch location for a notched component subjected to the multiaxial cyclic loading, a cyclic plasticity model has to be related with the equation set, equation (31). In several past decades, many plasticity models have been developed to model the material behavior using different levels of complexity from simple to complicated solutions. Modeling complex material behavior such as cyclic hardening/softening, ratcheting and nonproportional hardening requires extensive material testing to determine material constants required for the modeling of complex material behaviors. It is intended in this article to focus on a plasticity model for its simplicity and efficiency to characterize the material stress–strain responses with a reasonable accuracy. Such a plasticity model is considered to be suitable for the multiaxial stress–strain notch analysis. The differences in the plasticity models are generally based on the translation rule that governs the movement of the yield surface. One of the most popular cyclic plasticity models was proposed by Mroz.[23] Mroz defined a field of plastic moduli in stress space for better approximation of the stress–strain curve and generalization of the plastic modulus in multiaxial case. Each surface is represented by its center coordinates a_{ij}^{k}, a yield stress σ_{yo}^{k} and a plastic modulus $E_{t}^{p(k)}$. If the von Mises criterion is used to represent the surface, the yield surface is defined as

$$F^{k}(S_{ij}, a_{ij}) = \frac{3}{2}\left(S_{ij} - a_{ij}^{k}\right)\left(S_{ij} - a_{ij}^{k}\right) - \sigma_{yo}^{k} 2 = 0 \tag{41}$$

Garud[21] showed a possibility of intersecting yield surfaces for Mroz model under certain loading; therefore, Garud proposed an improved translation rule that prevents any intersections of plasticity surfaces. Garud suggested that the movement of the stress surface depends not only on the current state of stress but also on the direction of stress increment. Garud postulated that increases in stress induce the evolution of plastic deformation, and the surfaces are subject to translation, keeping constant shape and size without rotation in the stress space. The assumed direction of movement provides locations of the current state of stress on the surface at the new location and eliminates the possibility of intersection between adjacent surfaces. The

principle idea of the Garud translation rule is demonstrated in the following steps.

It is assumed that an applied load results in the current stress state settled at the point S and the two yield surfaces F_1 and F_2 with the corresponding yield limits R_{F1} and R_{F2} have been moved in the stress space, so that their centers have been located to the points a_{ij}^{F1} and a_{ij}^{F2} as it has been arbitrarily assumed and illustrated in Figure 8.

Based on the applied load path, the current stress increment induces the plastic strain increment, and it is forwarded outside the surface F_1. According to the consistency condition, the yield surface must follow the stress state evolution, and the updated stress state $S_{ij} + \Delta S_{ij}$ must satisfy the updated yield function $F_1(S_{ij} + \Delta S_{ij} - a_{ij}^{F1} - \Delta a_{ij}^{F1}) - R_{F1} = 0$. During the plastic strain evolution the yield surface with a fixed size R_{F1} translates without rotation in the stress space. Taking into account this assumption that the consistency condition is satisfied by the condition as the surface centered at the point $S_{ij} + \Delta S_{ij}$ corresponding to the updated stress state

$$F_1[(a_{ij}^{F1} + \Delta a_{ij}^{F1}) - (S_{ij} + \Delta S_{ij})] - R_{F1} = 0 \tag{42}$$

Thus, the translation rule of the yield surface must be defined. The details of the yield surface translation rule according to Garud's proposition are discussed in the following. The translation is associated with the applied load path that generates a plastic strain evolution.

In order to translate the yield surface according to the Garud rule, the following steps should be performed.

(a) Extend the current stress increment to intersect the next inactive yield surface F_2 at the point A_2 as it is presented in Figure 8.

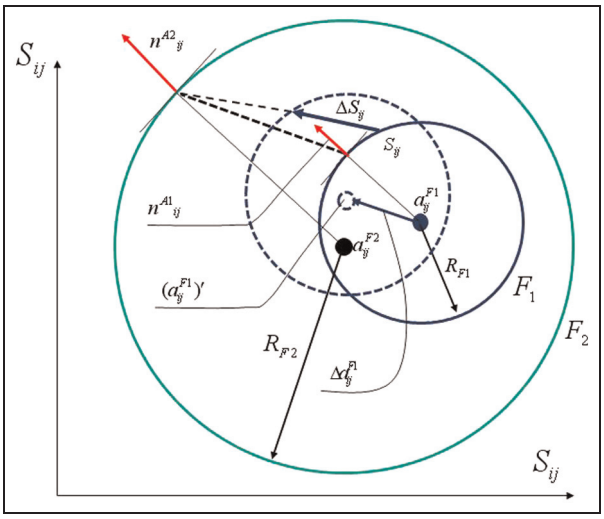

Figure 8. A graphical representation of the Garud cyclic plasticity model.

In the index notation, the following equation describes the present step

$$\left|\overline{S_{ij} + x \cdot \Delta S_{ij} - a_{ij}^{F2}}\right| = R_{F2} \tag{43}$$

where the unknown coordinates of the point A_2 are expressed as

$$S_{ij}^{A2} = S_{ij} + x \cdot \Delta S_{ij} \tag{44}$$

Find a normal vector on the next surface at the point of intersection

$$n_{ij}^{A2} = \sqrt{\frac{3}{2}} \frac{S_{ij}^{A2} - a_{ij}^{F2}}{R_{F2}} \tag{45}$$

(b) Determine a point A_1 on the active surface F_1 with the same normal vector.

The two operations are described in the index notation in the following form

$$\begin{aligned} n_{ij}^{A2} &= n_{ij}^{A1} = \sqrt{\frac{3}{2}} \frac{S_{ij}^{A1} - a_{ij}^{F1}}{R_{F1}} \\ S_{ij}^{A1} &= \frac{R_{F1}}{R_{F2}} \left(S_{ij}^{A2} - a_{ij}^{F2}\right) + a_{ij}^{F1} \end{aligned} \tag{46}$$

(c) Connect the conjugate points A_1 and A_2 to find the direction of translation of the yield surface F_1, as shown in Figure 8 (current yield surface moves in the direction of the connection between two normal vectors)

$$(\overline{A_1 A_2})_{ij} = S_{ij}^{A2} - S_{ij}^{A1} \tag{47}$$

(d) Translate the surface F_1 from point a_{ij}^{F1} to $(a_{ij}^{F1})'$ in the direction of the vector $(A_1\ A_2)$ till the stress increment ΔS_{ij} is found on the translated surface, as presented in Figure 8.

In terms of the index notation, the following equation can be defined

$$\left|\overline{S_{ij} + \Delta S_{ij} - a_{ij}^{F1} - \Delta a_{ij}^{F1}}\right| = R_{F1} \tag{48}$$

in which the components Δa_{ij}^{F1} of the translation vector are expressed

$$\Delta a_{ij}^{F1} = y\left(S_{ij}^{A2} - S_{ij}^{A1}\right) \tag{49}$$

Thus, the updated coordinates of the center of the yield surface F_1 are given as

$$(a_{ij}^{F1})' = a_{ij}^{F1} + \Delta a_{ij}^{F1} \tag{50}$$

The yield surface movement is determined by calculating the scalar parameter y defined by the consistency condition represented by equation (48). Barkey[14] and

Singh[17] utilized Mroz's multisurface plasticity model for the notch-tip stress and strain calculations. However, it is found that Mroz and Garud's plasticity model produces identical stress–strain predictions when a number of plasticity surfaces exceeded a certain value and a loading increment is infinitesimal. Otherwise, for the finite loading increment, the intersection of plasticity surfaces occurs in the Mroz model, and the Garud model generates more accurate stress–strain results than the Mroz model.

Numerical implementation

The elastic–plastic stress–strain model consists of two parts, namely, the Garud cyclic plasticity model and the multiaxial Neuber notch correction rule to compute the actual elastic–plastic stress–strain response at notches using the FE linear elastic stress data. In order to implement equations defined in this article for a notched component subjected to multiaxial cyclic loads, a general numerical algorithm has been developed. The flowchart of the algorithm is shown in Figure 1. The algorithm starts with the linear elastic FEA results of a notch component for unit loads (a macro written in APDL is used to output linear elastic solution for each unit load). In the next step, two separate computer programs written in Fortran 90 are used performing the elastic–plastic stress–strain analysis; the first computer program is used to superimpose linear elastic stress histories at notch region of the FE model subjected to multiaxial loads and the second computer program is used to implement the notch stress and strain analysis using increments of linear elastic stress histories (output from the first program).

For the implementation of the first program, the linear elastic FE results for each unit load are multiplied by the corresponding load history to compute elastic stress history for that applied load history, and then the elastic stress histories for all applied load histories are superimposed to obtain the combined time histories of linear elastic stresses in accordance with equations (5)–(7). The resultant elastic stress history for each node at the critical notch region is divided into small increments of stresses for numerical implementation of elastic–plastic stress–strain analysis (Figure 4).

The second program computes the actual elastic–plastic stress and strain responses at notch areas. In the beginning of the program, loading criterion conditions must be checked. The yield surfaces are initially centered at the origin (no loading) and all stresses are assumed to be elastic, the stress–strain solution being determined by equation (9). When the elastic loading reached the initial yield surface, unloading criterion, equation (40), is used to determine elastic unloading/tangential loading and elastic–plastic loading during state of stress increment. If the elastic–plastic loading takes place, the actual elastic–plastic strain and stress increments are calculated using equation (31). A set of seven equations (three notch correction equations from Neuber's rule and four constitutive equations) is solved simultaneously to determine the actual elastic–plastic strain and stress increments. Then, the active surfaces are translated according to equations (42)–(50). If stresses exceed the outer yield surface as governed by equation (43), the stress increment is bisectioned, and then stresses are updated to the point where new stress state lies on the yield surface. The current state of the active surface is also updated. The elastic–plastic stress–strain calculation is repeated for the remaining portion of stress increments. If the stresses after the load increment remain on the current active yield surface, the stresses are updated and the active surface and any interior surfaces are translated. The procedure is repeated until the last elastic stress increment is reached.

One critical part of the actual stress–strain calculation is based on the cyclic plasticity model. The cyclic plasticity model is used to determine the active yield surface, which is necessary to define the parameter $d\lambda$ in the governing equation (25). In other words, the plasticity model determines which piece of the stress–strain curve (the slope of the actual stress–strain curve) has to be utilized for given stress/load increment $\Delta\sigma_i$ to define the plastic modulus $\Delta\sigma_{eq}/\Delta\varepsilon^p_{eq}$. The plasticity models are generally used for calculating stress or strain increments that result from given stress–strain elements. In the case of the notch analysis, neither stresses nor strains are direct inputs to the plasticity model. The input is provided in the form of the total deviatoric strain energy density increments, and both the actual deviatoric stress and strain increments ΔS^a_{ij} and Δe^a_{ij} are unknowns, and these unknown stress and strain increments are simultaneously calculated by solving the equation set, equation (31). After calculating the deviatoric stress increments ΔS^a_{ij}, the plasticity surfaces are translated as shown in Figure 8. The calculated deviatoric stress increments ΔS^a_{ij} are subsequently converted into the actual stress increments $\Delta\sigma^a_{ij}$ using equation (32).

The process is repeated for each subsequent increment of the "elastic" input $\Delta\sigma^e_{ij}$. The cyclic plasticity model assumes a stable material response such that no transient hardening effects of the nonproportional hardening are taken into account.

Results and discussion

In order to predict the fatigue failure of notched components under the multiaxial cyclic loadings, it is essential to provide a good understanding of how external loads relate to the state of stress and strain at the critical location and material constitutive behavior. To establish the prediction capability of the notch stress and strain analysis model presented in this investigation, calculated elastic–plastic notch strains and stresses obtained from the elasto-plastic stress–strain model are compared to the experimental strain and stress data of

SAE 1070 steel notched bar for six different nonproportional load paths.[14] Pseudo-elastic stress histories for each load path were calculated using linear elastic FE stress results. Calculated elastic stress histories are then used as input to the analytical elasto-plastic notch analysis model to compute actual elastic–plastic strains and stresses at the critical notch area.

Barkey[14] performed experiments on circumferential notched shafts subjected to various nonproportional load paths. The notched shafts were subjected to cyclic tension and torsional load histories under conditions of load controls by using Instron and MTS tension–torsion biaxial test frames. Strain gauges were mounted on the notch root for strain measurements. The experimented notch shafts were a cylindrical bar with a circumferential notch similar to that shown in Figure 5. Each cylindrical specimen was machined from SAE 1070 steel stack to the proper geometry, then heat treated to give uniform material properties. The actual radius of the cylindrical specimen was $R = 25.4\,\text{mm}$, and notch dimensions of the cylindrical specimen were $\rho/t = 1$ and $R/t = 2$. The FEA and experimental stress concentration factors are listed in Table 1. These stress concentration factors are relatively mild and would exist on typical notched components such as those found in many ground vehicle applications. The ratio of the measured notch-tip hoop stress to the axial stress under tensile axial loading was $\sigma^e_{33}/\sigma^e_{22} = 0.184$.

The FE model for the analyzed notched shaft is shown in Figure 9. The geometry of the notched shaft was modeled in ANSYS FE code and then meshed using three-dimensional (3D) hexagonal (brick) solid elements, and the area near the notch root was carefully refined as shown in Figure 9 to obtain accurate pseudo-elastic stress tensors at the notch location. The pseudo-elastic stress σ^e_{ij} tensors obtained from the FE model are based on the cylindrical coordinate system that is defined as: y axis is the primary axial axis, z axis is the tangent to the notch surface and x axis is perpendicular to the notch. The coordinate system x-y-z defined for the FE model is interchangeably used as 1-2-3 coordinate system for the stress and strain tensors. Linear elastic tensors (nodal stresses on the critical notch area) for the applied load paths were read and converted (using the computer program) to a format readable by the elastic–plastic stress–strain model. Linear elastic stress results from two unit load cases (axial and torsion) were combined with actual axial and torsion load paths using the principle of superposition to obtain increments of pseudo-elastic stress histories. The increments of hypothetical "elastic" stress components σ^e_{22}, σ^e_{33} and σ^e_{23} were used as input for the analytical elastic–plastic stress–strain model.

The material for the notched bar was SAE 1070 steel with a cyclic stress–strain curve (Figure 10) approximated by the Ramberg–Osgood relation. The material properties were given as $E = 210\,\text{MPa}$, $\nu = 0.3$, $S_Y = 242\,\text{MPa}$, $n' = 0.199$ and $K' = 1736\,\text{MPa}$.

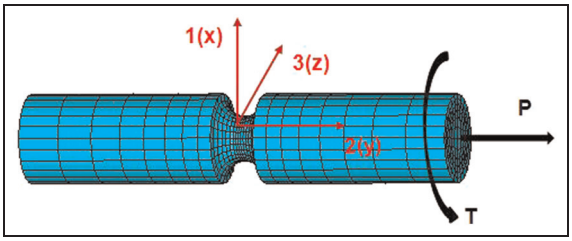

Figure 9. FEA model for SAE 1070 steel notched specimen.

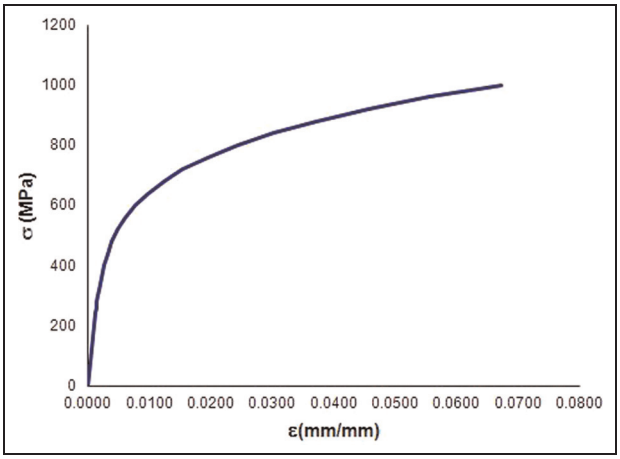

Figure 10. SAE 1070 cyclic stress–strain curve.

Table 1. FEA and experimental stress concentration factors of SAE 1070 notched bar.

	σ^e_{22}/σ_n	σ^e_{33}/σ_n	σ^e_{23}/σ_n
FEA	1.42	0.30	1.15
Experiment	1.41	0.26	1.15

FEA: finite element analysis.

Pseudo-elastic notch stresses, σ^e_{22}–σ^e_{23}, for clockwise and counterclockwise box-shaped cyclic stress paths are shown in Figures 11 and 12, respectively. The clockwise/counterclockwise box-shaped load paths were repeated more than 100 cycles while recording the strains at the notch tip. The box path indicates a high degree of nonproportionality loading. This load path was designed to show regions that axial and shear responses are uncoupled (elastic response) and where they are coupled (elastic–plastic response). Therefore, the box-shaped load path provides a critical test for the proposed stress–strain model for notch-tip strain and stress calculations. The maximum nominal tensile and torsion stresses were $\sigma_n = 296\,\text{MPa}$ and $\tau_n = 193\,\text{MPa}$, respectively. The corresponding pseudo-elastic notch stresses were $\sigma^e_{22} = 417.3\text{MPa}$ and $\sigma^e_{23} = 221.9\text{MPa}$, respectively. Comparison of the measured and calculated notch strain responses for the clockwise and counterclockwise box-shaped load paths is shown in

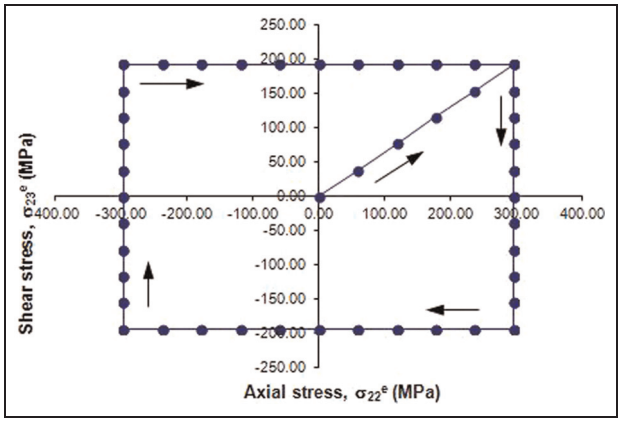

Figure 11. Box cyclic stress–load path—clockwise.

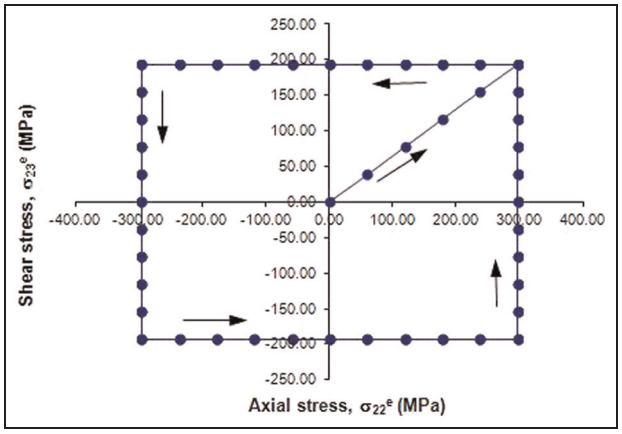

Figure 12. Box cyclic stress–load path—counterclockwise.

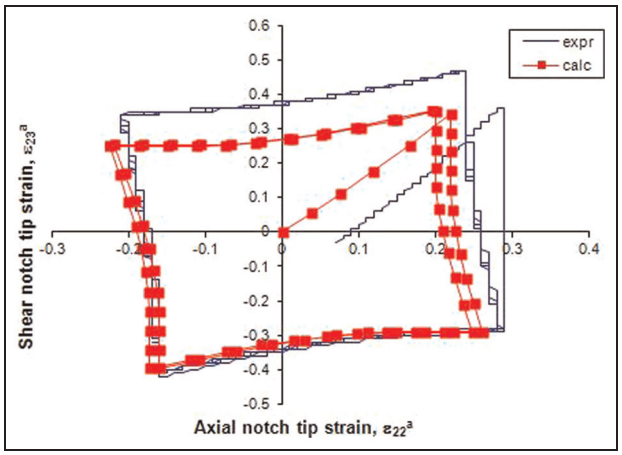

Figure 13. Experimental and calculated strain paths in the notch tip induced by the box input loading path—clockwise.

Figures 13 and 14, respectively. It can be noted that the agreement between the calculated and measured strain responses are qualitatively and quantitatively good. The strain paths show deviation from the box-shaped load paths at the onset of local plasticity for both the

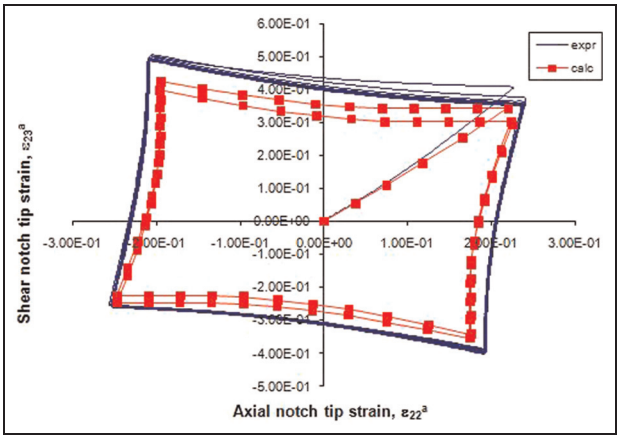

Figure 14. Experimental and calculated strain paths in the notch tip induced by the box input loading path—counterclockwise.

experiment and the model. It can also be seen from Figures 13 and 14 that the proposed elastic–plastic stress–strain model predicts the elastic unloading at each corner of the box (the axial and shear strains are uncoupled) and followed by the elastic–plastic response to the next corner (the axial and shear strains are coupled). Figures 13 and 14 also indicate that the strains ranges are predicted as approximately 5%–15% smaller than experimental ones. These underestimations in strain ranges might result in nonconservative fatigue life predictions.

Several nonproportional cyclic loading paths during which ratios of the frequency of applied loads were unequal were applied to the notched-bar specimen. The maximum nominal stresses were $\sigma_n = 296\,\text{MPa}$ and $\tau_n = 193\,\text{MPa}$. Nonproportional load paths from unequal frequencies of applied loads are a common type of loadings experienced by many machine components. Four of those load paths at unequal frequencies of tensile to torsional load paths in the ratio of 3:1, 5:1, 1:3 and 1:5 are analyzed here. Three cycles of tensile load were applied in the same time period as one cycle of torsional load (Figure 15). Five cycles of tensile load were applied in the same time period as one cycle of torsional load (Figure 16). Three cycles of torsional load were applied in the same time period as one cycle of tensile load (Figure 17). Five cycles of torsional load were applied in the same time period as one cycle of tensile load (Figure 18). Axial and shear strain histories obtained from the model and experiments are plotted in Figures 19–22 for the tensile to torsional frequency ratios of 3:1, 5:1, 1:3 and 1:5, respectively. As seen from these figures that there are slight offsets between the measured strain paths and the calculated strain paths, which were obtained from the stabilized cyclic stress–strain curve. The offsets might be attributed to the fact that the measured strain paths are not symmetric with respect to the center of coordinates during the first

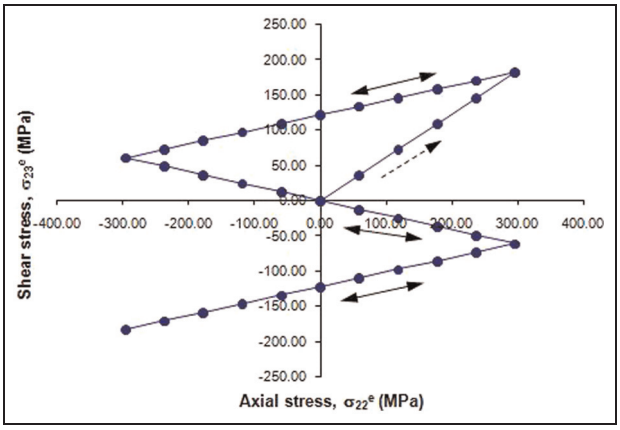

Figure 15. Unequal frequency (ratio 3:1) tension–torsion stress/loading path.

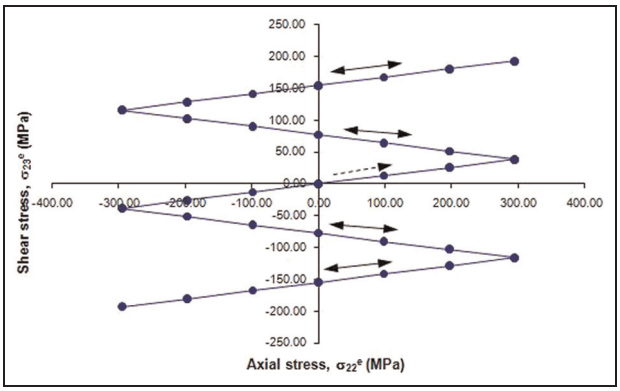

Figure 16. Unequal frequency (ratio 5:1) tension–torsion stress/loading path.

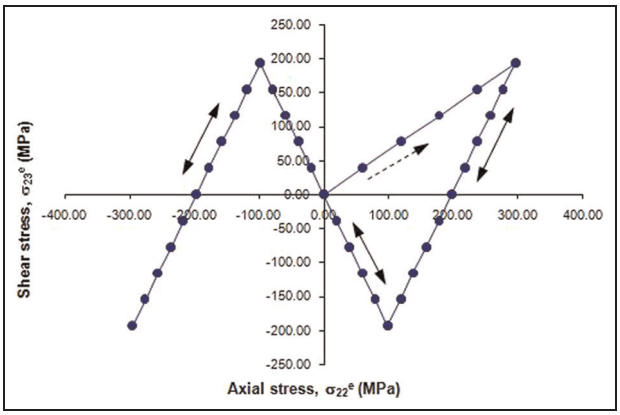

Figure 17. Unequal frequency (ratio 1:3) tension–torsion stress/loading path.

cycle, which are always slightly different from the subsequent cyclically stabilized material response, might cause the shift of the strain responses. In spite of this offset, strain responses computed by the elastic–plastic stress–strain model reasonably agree well with the experiment results in terms of the general trend and numerical strain values.

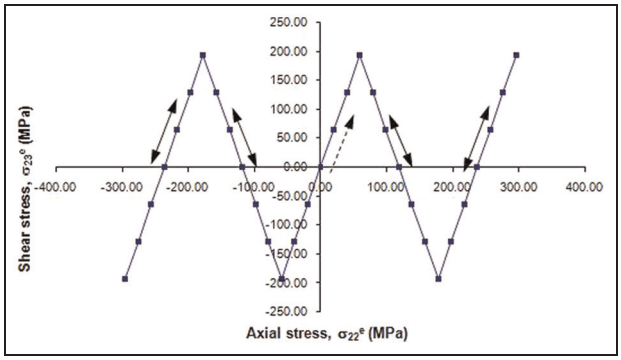

Figure 18. Unequal frequency (ratio 1:5) tension–torsion stress/loading path.

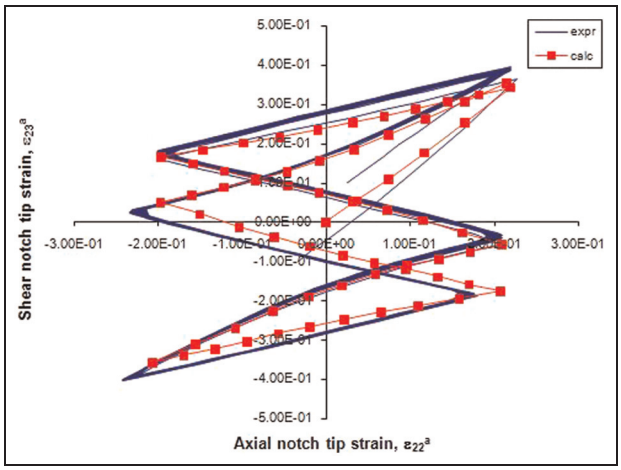

Figure 19. Experimental and calculated strain paths in the notch tip induced by the unequal frequency (ratio 3:1) tension–torsion input loading path.

Conclusion

In this article, the simple analytical multiaxial notch analysis model, which is based on the Garud cyclic plasticity model integrated with the multiaxial Neuber correction rule, has been developed to estimate the elastic–plastic notch-tip material behavior of the notch components subjected to the multiaxial nonproportional loadings using linear elastic FE stress solution.

In order to determine the predictive accuracy of the multiaxial elasto-plastic notch analysis model, the model was validated against the experimental results of SAE 1070 steel notched shaft obtained by Barkey. Based on the comparison between the experimental and computed strain histories for six different nonproportional load paths, the elastic–plastic stress–strain model predicted notch strains with reasonable accuracy using linear elastic FE stress histories.

The implementation of the incremental strain energy density equations in the deviatoric stress space and the utilization of the Garud plasticity model provided more accurate notch-tip stress–strain calculations than previously suggested strain energy density approaches by Moftakhar et al.[12] Barkey[14] and Singh.[17]

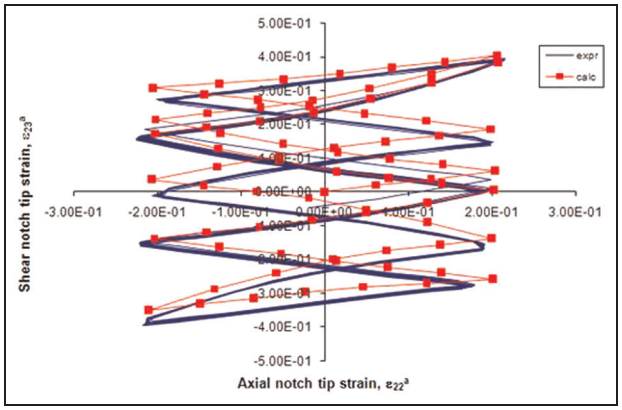

Figure 20. Experimental and calculated strain paths in the notch tip induced by the unequal frequency (ratio 5:1) tension–torsion input loading path.

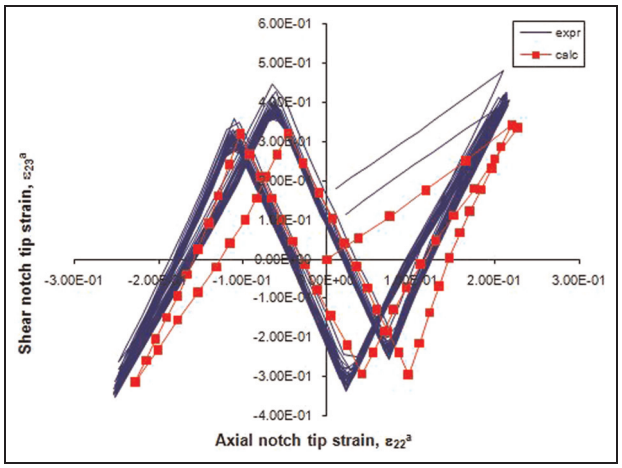

Figure 21. Experimental and calculated strain paths in the notch tip induced by the unequal frequency (ratio 1:3) tension–torsion input loading path.

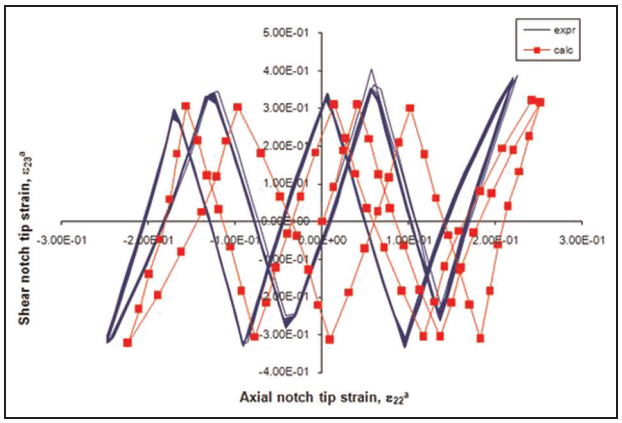

Figure 22. Experimental and calculated strain paths in the notch tip induced by the unequal frequency (ratio 1:5) tension–torsion input loading path.

The multiaxial elasto-plastic stress–strain model developed in this article provides a more efficient and logical analytical approach to estimate notch-root elastic–plastic stress and strain responses for the notch component under the multiaxial nonproportional loading. For this reason, the multiaxial notch analysis model may be employed to perform fatigue life estimation for the notched components subject to complex multiaxial loadings. The effect of changes in material, geometry and loads on the fatigue life can then be assessed in a short time frame in practical engineering applications; thus, the design of notched components can be evaluated and optimized for the service life in the early design phase.

Funding

This research received no specific grant from any funding agency in the public, commercial, or not-for-profit sectors.

References

1. Peterson RE. *Stress concentration factors*. New York: John Wiley & Sons, 1977.
2. Stowell EZ. *Stress and strain concentration at a circular hole in an infinite plate*. NACA Technical Report 2073, April 1950. Washington, DC: NACA.
3. Hardrath HF and Ohman H. *A study of elastic plastic stress concentration factors due to notches and fillets in flat plate*. NACA Technical Report 2566, December 1951. Washington, DC: NACA.
4. Neuber H. Theory of stress concentration for shear strained prismatic bodies with arbitrary stress–strain law. *J Appl Mech* 1961; 28: 544–550.
5. Topper TH, Wetzel RM and Morrow JD. Neuber's rule applied to fatigue of notched specimens. *J Mater* 1969; 1: 200–209.
6. Molski K and Glinka G. A method of elastic-plastic stress and strain calculation at a notch root. *Mater Sci Eng* 1981; 50: 93–100.
7. Glinka G. Energy density approach to calculation of inelastic strain–stress near notches and cracks. *Eng Fract Mech* 1985; 22: 485–508.
8. Hoffmann M and Seeger T. A generalized method for estimating multiaxial elastic–plastic notch stresses and strains. Part I: theory. *J Eng Mater: T ASME* 1985; 107: 250–254.
9. Hoffmann M and Seeger T. Stress–strain analysis and life predictions of a notched shaft under multiaxial loading. In: Leese GE and Socie D (eds) *Multiaxial fatigue: analysis and experiments AE-14*. Warrendale, PA: Society of Automotive Engineers, 1989, pp.81–101.
10. Ellyin F and Kujawski D. Generalization of notch analysis and its extension to cyclic loading. *Eng Fract Mech* 1989; 32(5): 819–826.
11. Moftakhar AA. *Calculation of time independent and time-dependent strains and stresses in notches*. PhD Dissertation, Department of Mechanical Engineering, University of Waterloo, Waterloo, ON, Canada, 1994.
12. Moftakhar A, Buczynski A and Glinka G. Calculation of elasto-plastic strains and stresses in notches under multiaxial loading. *Int J Fracture* 1995; 70: 357–373.
13. Hoffmann M, Amstutz H and Seeger T. Local strain approach in non-proportional loadings. In: Kussmaul K,

McDiarmid D and Socie D (eds) *Fatigue under biaxial and multiaxial loadings—ESIS 10*. London: Mechanical Engineering Publications, 1991, pp.357–376.
14. Barkey ME. *Calculation of notch strains under multiaxial nominal loading*. PhD Dissertation, University of Illinois at Urbana-Champaign, Urbana, IL, 1993.
15. Barkey ME, Socie DF and Hsia KJ. A yield surface approach to the estimation of notch strains for proportional and non-proportional cyclic loading. *J Eng Mater: T ASME* 1994; 116: 173–180.
16. Köttgen VB, Schoen M and Seeger T. Application of multiaxial load-notch strain approximation procedure to autofrettage of pressurized components. In: McDowell DL and Ellis R (eds) *Advances in multiaxial fatigue, ASTM STP 1191*. Philadelphia, PA: American Society for Testing and Materials, 1993, pp.375–396.
17. Singh MNK. *Notch tip stress-strain analysis in bodies subjected to non-proportional cyclic loads*. PhD Dissertation, Department of Mechanical Engineering, University of Waterloo, Waterloo, ON, Canada, 1998.
18. Köttgen VB, Barkey ME and Socie DF. Pseudo stress and pseudo strain based approaches to multiaxial notch analysis. *Fatigue Eng Mater* 2001; 34: 854–867.
19. Buczynski A and Glinka G. Elastic-plastic stress-strain analysis of notches under non-proportional loading paths. In: F Ellyin and JW Provan (eds) *Proceedings of the international conference on progress in mechanical behaviour of materials (ICM8)*, Victoria, BC, Canada, 16–21 May 1999, vol. 3, pp.1124–1130.
20. Ye D, Hertel O and Vormwald M. A unified expression of elastic-plastic notch stress-strain calculation in bodies subjected to multiaxial cyclic loading. *Int J Solids Struct* 2008; 45: 6177–6189.
21. Garud YS. A new approach to the evaluation of fatigue under multiaxial loadings. *J Eng Mater: T ASME* 1981; 103: 118–125.
22. Drucker DC. A more fundamental approach to plastic stress-strain relation. In: *Proceedings of the first U.S. congress of applied mechanics*, Chicago, USA, June 1951, pp.487–491. New York: ASME.
23. Mroz Z. On the description of anisotropic workhardening. *J Mech Phys Solids* 1967; 15: 163–175.
24. Chu CC. A three-dimensional model of anisotropic hardening in metals and its application to the sheet metal forming. *J Mech Phys Solids* 1984; 32(3): 197–212.
25. Amstrong PJ and Frederick CO. *A mathematical representation of the multiaxial Bauschinger effect*. Central Electricity Generating Board. Technical Report RD/B/N 731, 1966. UK: Berkeley Nuclear Laboratories, Research and Development Department.
26. Chaboche JL. Time-independent constitutive theories for cyclic plasticity. *Int J Plasticity* 1986; 2(2): 149–188.
27. Jiang Y and Kurath P. A theoretical evaluation of plasticity hardening algorithms for nonproportional loading. *Acta Mech* 1996; 118: 213–234.